Instrument and methods for surface dilatational rheology measurements

Stoyan C. Russev,[1] Nikola Alexandrov,[2] Krastanka G. Marinova,[2,a)] Krassimir D. Danov,[2] Nikolai D. Denkov,[2] Lyudmil Lyutov,[3] Vassil Vulchev,[4] and Christine Bilke-Krause[5]
[1]*Department of Solid State Physics, Faculty of Physics, University of Sofia, Sofia 1164, Bulgaria*
[2]*Laboratory of Chemical Physics and Engineering, Faculty of Chemistry, University of Sofia, 1164 Sofia, Bulgaria*
[3]*Department of General and Inorganic Chemistry, Faculty of Chemistry, University of Sofia, Sofia 1164, Bulgaria*
[4]*Department of General Physics, Faculty of Physics, University of Sofia, Sofia 1164, Bulgaria*
[5]*KRÜSS GmbH, Wissenschaftliche Laborgeräte, 22453 Hamburg, Germany*

(Received 22 February 2008; accepted 24 September 2008; published online 27 October 2008)

We describe an instrument combining the advantages of two methods, axisymmetric drop shape analysis for well-deformed drops and capillary pressure tensiometry for spherical drops, both used for measuring the interfacial tension and interfacial rheological parameters. The rheological parameters are the complex interfacial elasticity, and the surface elasticity and viscosity of Kelvin–Voigt and Maxwell rheological models. The instrument is applicable for investigation of the effect of different types of surfactants (nonionic, ionic, proteins, and polymers) on the interfacial rheological properties both of air/water and oil/water interfaces, and of interfaces between liquids with equal mass densities. A piezodriven system and a specially designed interface unit, implemented in the instrument, ensure precise control for standard periodic waveforms of surface deformation (sine, square, triangle, and sawtooth) at a fixed frequency, or produce surface deformation at constant rate. The interface unit ensures accurate synchronization between the pressure measurement and the surface control, which is used for real-time data processing and feedback control of drop area in some of the applications. © *2008 American Institute of Physics.* [DOI: 10.1063/1.3000569]

I. INTRODUCTION

Interfacial properties (dynamic and equilibrium interfacial tension and dilatational rheological parameters) are among the main factors determining the dynamic behavior of foams and emulsions.[1–4] Foam drainage[2] and foam rheology[3] have been shown to correlate with the surface dilatational modulus. It has been suggested also[1,4] that the stability of foams and emulsions depends on the surface rheological properties but no firm evidences have been found so far.[5] Therefore methods and procedures for determination of the interfacial tension, interfacial elasticity, and viscosity have been subjects of a significant development and investigations for years.[4,6–17]

In the last 30 years one of the most popular methods for interfacial tension measurements has become the calculation of interfacial tension by fitting the axisymmetric profile of well-deformed drops or bubbles with the numerical solution of Laplace equation of capillarity. This method is known as the axisymmetric drop shape analysis (DSA).[8,9] Soon after the implementation of DSA for equilibrium measurements, the method has been further developed and applied for surface dilatational rheology measurements.[10] In many cases the new method complemented and even replaced the more complex and difficult for realization method with Langmuir trough.[10–12] Working with small drops in the case of DSA instead with large volumes and surfaces (needed for the Langmuir trough) has the advantages of using small quantities (important for expensive samples and biological specimens), and relatively easy and fast replacement of the tested volume and renewal of the surface studied.

Almost in parallel with the DSA methods, another group of methods, called the capillary pressure tensiometry (CPT), has been developed.[13–17] The CPT is based on the direct measurement of the capillary pressure difference across a spherical interface with a known radius of curvature. For measurements of the interfacial rheological parameters, CPT has been used in two versions: applying sine oscillations of the volume of bubbles[14] and drops[15] or producing continuous deformation (expansion or contraction) of drops.[16,17] The volume and the area of the drops and bubbles studied by CPT are about one order of magnitude smaller than those necessary for the DSA measurements. The smaller drop volume and the faster calculation of the interfacial tension (due to the faster pressure detection and simpler calculation procedures) allow application of the CPT method at considerably higher frequencies. This is the only method for dilatational rheology which can be used for liquids with small density difference, when it is impossible to form sufficiently deformed drops for DSA. In spite of these advantages, the CPT setups have been developed and used until recently only for laboratory scientific investigations due to the relatively complex and time consuming calibration procedures.

[a)]Author to whom the correspondence should be addressed. Electronic mail: km@lcpe.uni-sofia.bg.

In this paper we describe an instrument, which works with small drops and bubbles, and allows measurements of the interfacial tension and dilatational rheological properties (see also Ref. 18). The apparatus combines the methods and advantages of both DSA and CPT. The interfacial rheological behavior can be studied either by applying one of the standard periodic surface deformations (sine, square, triangle, and sawtooth) or with constant rate of surface deformation. A special interface unit (IU) is developed for a precise time control and detection of the processes with time synchronization better than 10 μs. Thus the periodic surface deformation can be realized with a frequency up to 100 Hz. The upper frequency limit of the measurements is currently restricted by the frequency of the interfacial tension detection—25 Hz for a standard charge coupled device (CCD) camera and 1000 Hz for the used pressure transducer. It is possible to use a high-speed camera, allowing even 5000 Hz registration; however we restricted our test measurements up to 1 Hz because the viscosity effects should be especially accounted for at higher frequencies, even when working with standard systems (water or mineral oils).[19] Details for the construction, software, and the procedures are given in Sec. II. In Sec. III we illustrate the application of the instrument. First, we performed measurements on several systems, which are widely studied in literature and compare our results with the results obtained by other authors. Next, to demonstrate the advantages of the described instrument we studied also several other systems (containing viscous oil phases and/or liquids with small density difference), which to the best of our knowledge, have not been studied so far by other authors because of the technical difficulties encountered by the existing methods.

II. EXPERIMENT

A. Instrument and assembly software

Figure 1 presents schematically the used setup, which consists of the following main parts: (A) hardware for drop or bubble formation and volume control (filling system); (IU) interface unit for pressure data acquisition and volume control; (B) system for video observation; and (PC) computer with software for signals processing and interfacial tension calculations. The video system of the commercially available instrument for contact angle determination and DSA10 (Krüss GmbH, Hamburg, Germany) was used, along with the software DSA1 for calculation of the interfacial tension of well-deformed drops and bubbles.

1. Hardware construction

We developed a special hardware construction (A) for drop (bubble) formation and control, illustrated in Fig. 1. The drop (1) is formed on the tip of a needle (2) attached to the filling system. The filling system contains the fluid(s), from which the drop (bubble) is formed, and it consists of a compartment with a metal membrane sealed to a piezotransducer (3) and a syringe (4). All parts of the filling system are made from stainless steel, glass, or Teflon. The stainless steel holder of the piezodriven membrane is equipped with a glass window to ensure a visual inspection for the presence of air bubbles in the inner fluid. Standard needles from stainless steel or glass are used. Two three-way valves (5) connect the compartment with the needle and the syringe. The pressure transducer (6) is connected to the system through the three-way valve just above the needle. The used plugging valves are of HVP model (Hamilton, USA) with chemically inert Teflon® and Kel-F® inner parts.

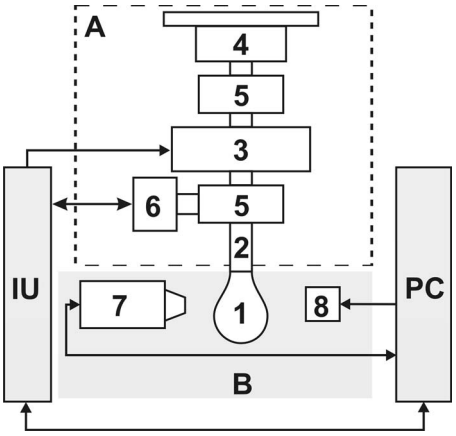

FIG. 1. Schematic of the instrument for surface rheological studies. (a) A drop or bubble (1) is formed on the tip of a needle (2). The needle is attached to a filling system comprising a block with a piezodriven membrane (3), manually controlled syringe (4) and valves (5). Differential pressure transducer (6) is also connected to the system. (b) The drop (bubble) is observed in transmitted light by means of the video camera (7) and illumination (8). The image is processed with a computer (PC) having a frame grabber and suitable software (DSA1 from Krüss GmbH in our case). Specially developed IU controls the piezodriver and amplifies the signal from the pressure transducer.

The hardware construction is firmly attached to a supporting plate, mounted on the base of the DSA10 instrument. The drop (bubble) is observed in transmitted light by means of the camera (7) and the illumination system (8) built in the DSA10 instrument. The piezotransducer is controlled by specially designed IU. All processes are controlled by specially developed software, installed on the personal computer (PC).

2. Interface unit

Figure 2 shows the block diagram of the IU. The IU is connected to the PC through a standard USB interface,[20] which maintains a fast bidirectional interchange of data. Additional RS-232 interface connection is available, which is used only for downloading the microcontroller embedded

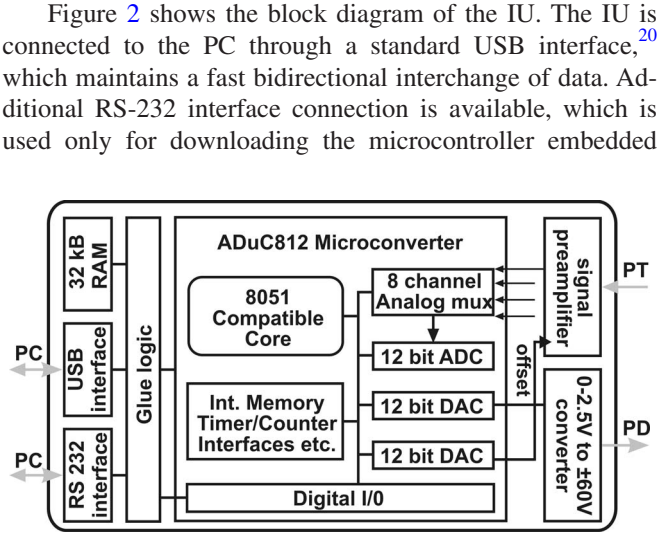

FIG. 2. Block diagram of the IU, in which PT states for the pressure transducer and PD—for the piezodriver.

program and is not used during the actual work of the system. The IU secures one analog input for pressure data acquisition and two analog outputs—one is used for a drop volume control via piezotransducer and the other is for the user control of the pressure signal offset. The IU is based on fully integrated 12 bit data acquisition system ADUC812,[21] which incorporates on a single chip a high performance self-calibrating eight channel analog to digital converter (ADC), dual digital to analog converter (DAC), 8 bit 8051 instruction set compatible microcontroller core with 8 kB Flash/EE program memory, etc. Other functional blocks in the IU are USB and RS-232 interfacing blocks, 32 kB external random access memory (RAM), analog signals conditional blocks, and the "glue logic" between these components and the ADUC812 chip (Fig. 2).

The external 32 kB memory is used for storage of look-up table values, necessary for a fast generation of the desired waveform. The consecutive values of the look-up table are passed from the microcontroller at regular time intervals to DAC0, whose output reproduces desired waveform (Fig. 2). The numerical representations of the waveforms are precomputed by the main PC, rounded to integer values (12 bit resolution) and sent via USB to the IU, where the microcontroller stores them in the RAM look-up table. The internal timer/counter and interrupt routine are used for a precise timing of the waveform generation process. The time interval, at which DAC0 output is refreshed, is a parameter passed to the IU by the main PC, thus allowing a flexible control of the signal period. Another control parameter is an offset value, which the microcontroller adds to each sample point, thus ensuring a fast change of the drop volume during oscillations. DAC0 output range (0–2.5 V) is transformed to the voltage range of the piezotransducer (−60 V−+60 V) by the analog amplifier, which also ensures sufficiently high load capability output for driving capacitive loads. The used piezodriven membranes produce a maximal volume variation of ± 20 μl (end to end). When a desired waveform is realized, for example, sine oscillation, we use at least 1024 steps for peak-to-peak change. Typically the amplitudes of oscillations are from 0.1 to 5 μl (i.e., voltage oscillations from 0.3 to 15 V), which corresponds to 0.1 to 5 nl volume change in a single step.

An analog signal conditioning is also necessary to match the ADC input voltage range (0–2.5 V) to the pressure detector signal range. The output range of the pressure detector (Omega differential pressure transducer, model PX163-2.5BD5V) is 1–6 V. A quarter subrange of the total output range is selected by the software controllable offset and than amplified to fit the input range of the ADC. At full range of −621−+621 Pa, this gives 0.3 Pa step in recording the pressure signal (which is five times below typical noise of ± 1.5 Pa). The number of DAC reproduced points per period is also adjustable parameter. In the used working range (0.004–1 Hz), at least 1000 points per period are recorded, which ensures a precise reproduction of the desired drop volume change. Sine, square, triangle, and sawtooth waveforms with amplitude and offset control are included in the application program as standard options. At each point where the DAC output is changed, ADC samples, the pressure signal, and data are sent to the master PC. This ensures a constant phase shift of less than 10 μs between the driving signal points and the corresponding pressure data, thus simplifying the subsequent data treatment.

3. Software

The software comprises two parts: an application level program on the main PC; and a microcontroller embedded low-level program. Both programs communicate through USB protocol. Both main tasks of the system (the generation of waveforms and the recording of response signals) are time critical, which requires a careful distribution of the tasks between the main PC and the microcontroller. The time critical tasks for the real-time control and data acquisition are performed by the microcontroller program, while the application program implements a higher level control and ensures user-friendly interface. Both side double buffering guarantees a packet data exchange without introducing delays during the drop oscillations and data acquisition.

The microcontroller program is written in assembler and compiled with MetaLink's free 8051 Macro Assembler.[22] The Windows Serial Downloader (WSD.EXE) program[21] is then used to download via serial port the Intel standard hex file as created by the ASM51 assembler. The IU RAM is used for buffering the information necessary for the reproduction of the desired waveform and is filled in by the main PC via USB. The main PC also sends to IU the desired control parameters (time interval, waveform offset, pressure preamplifier offset, etc.) and switches it to the corresponding mode. The microcontroller reads from RAM consecutively each data record (2 byte), refreshes DAC0 output, reads ADC, and sends the samples back to the main PC. All timing is done using 16 bit timer/counter T2 of 8051 core and extensive use of the interrupts to ensure a maximum precision. The interrupt routine is used also for servicing USB data exchange using FT245 chip.[23]

The assembly program embedded in the microcontroller read-only memory encapsulates the real-time functionality of the system and leaves to the main PC program the general control of the system, imaging, edge detection, real-time data treatment, and data storage. For the communication of the application program with the IU via USB port, free drivers (D2XX) are available,[23] which allow FTDI devices to work with the most popular operating systems (LINUX, WINDOWS 98, and all higher versions). All function calls are encapsulated in standard DLL. This gives possibility to use different high level languages (C++, Visual Basic, Delphi, etc.) for writing the application program and ensures an easy communication with the IU via USB. In our case, the application programs are written in Delphi 7 including a well-designed interface for user-friendly control of the system parameters and modes of operation (period of oscillations, waveform, pressure preamplifier offset, etc.).

B. Procedures and application software

1. Drop/bubble formation

To start the experiment with *drop*, the entire filling system is filled with the desired internal liquid and afterward,

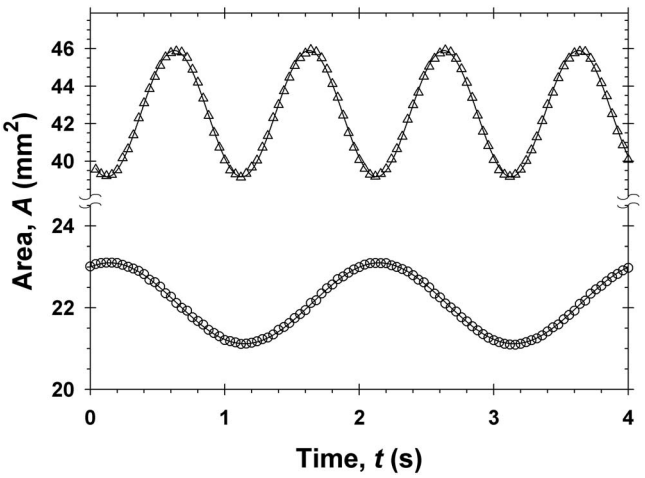

FIG. 3. Sine oscillations of the area of aqueous drop immersed in 5 mPa s PDMS with period of 1 s (triangles) and of aqueous drop in air with period of 2 s (circles). The solid lines are best fits to the data with the sine function $A_0+a_0\sin(\omega t+\varphi_A)$.

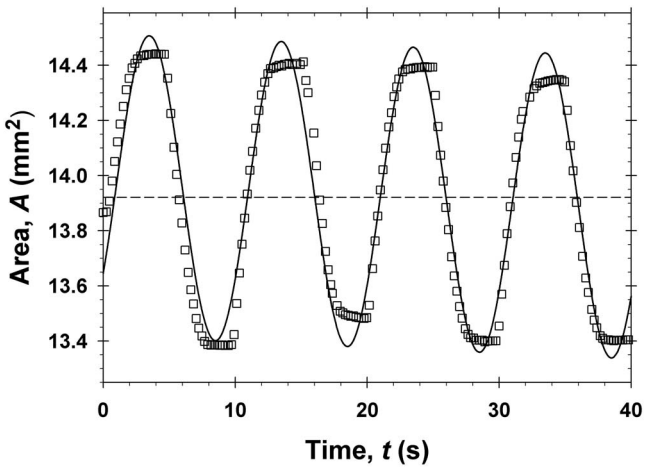

FIG. 4. Sine oscillations of the area of an aqueous drop in air with period 10 s, produced by a syringe-driven system.

one forms a drop on the tip of the needle by means of the syringe (see Fig. 1). Further fine tuning of the drop volume is performed by software controlled piezodriven membrane. The procedure for *bubble* formation is described in Ref. 24. Briefly, it consists in the following steps: first, we fill the needle and the system with pure water; afterward, we suck a small amount of air (from 50 to 100 μl) to fill the inner volume of the needle; third, the needle is dipped into the cuvette with a surfactant solution and the bubble is formed by pushing part of the air out of the needle either by using the syringe or the piezodriven membrane (see Fig. 1).

Three basic types of measurements are described below: (i) oscillating deformed drops or bubbles with pendant or sessile shapes (DSA); (ii) oscillating drops with spherical shapes [spherical drop analysis (SDA)]; and (iii) expanding/contracting spherical drops [expanding drop method (EDM)].

2. Oscillating deformed drops and bubbles

After the initial drop (bubble) formation, the user defines the control parameters of the desired waveform and starts the experiment. The system realizes drop oscillations, visualizes the drop shape, and stores the images in real time for subsequent data processing. The volume, V, area, A, and interfacial tension, σ, are calculated as a function of time, t, by fitting the solution of the Laplace equation to the drop (bubble) shape[8,9] using the software DSA1. Because sometimes the fitting procedure takes a long time, it is not performed during the measurement.

For small amplitudes of oscillations, the waveform of the area oscillations is assumed to be similar to the waveform of the volume oscillations. For example, we impose sine oscillations to the drops and bubbles by using a sine change in their volume with a fixed frequency, ω, through the piezodriven membrane (see Fig. 1). Good sine shape of area oscillations is obtained due to the precise volume control with small steps in short time intervals (Fig. 3). The solid lines in Fig. 3 represent the best fit of the experimental data $A(t)$ by sine function $A_0+a_0\sin(\omega t+\varphi_A)$, where A_0 is the initial drop area, a_0 is the amplitude of oscillations, and φ_A is the phase shift. Note that the parameters A_0 and ω are known and only two adjustable parameters, a_0 and φ_A, are determined from the fit. Excellent sine waveforms are illustrated in Fig. 3 also for a viscous outer phase [5 mPa s polydimethysiloxane (PDMS), see Sec. III A] and period 1 s. The decrease in the viscosity of the outer phase and the increase in the period of oscillations lead to more accurate sine waveforms.

Figure 4 illustrates the oscillations of an aqueous drop area with period of 10 s, obtained with a typical syringe-driven system taken from commercial instrument for DSA—the solid line represents the best sine fit of the experimental data. The comparison between the plots in Figs. 3 and 4 demonstrates that the shapes of the obtained area oscillations are much closer to the sine form for piezodriven system, as compared to the shape obtained with the syringe-driven system. This is not surprising, having in mind that our piezo-driven system changes the drop volume with nanoliter steps while such small volume changes are impossible with the currently available syringe-driven systems. Therefore, syringe-driven drop (bubble) oscillations have been used in literature only for periods longer than 5 s because significant deviations from the sine waveform are observed for shorter periods.[25] For this reason, we realize the drop deformation in our instrument by the piezodriven system only, whereas the syringe is used for formation of the initial drop.

Besides the sine oscillations, we implemented several other types of standard oscillations (square, triangle, and sawtooth) in the software. By controlling the driving voltage signal to the piezotransducer, we generate the desired shape of drop volume oscillations. The shape of area changes matches the shape of volume oscillations. Figure 5 shows an example for area oscillations with a triangle shape. The response of the surface tension to such types of area changes could be treated as described in Ref. 26, for example.

3. Oscillating spherical drops

When the mass density difference between the internal and external liquid phases is very small (viz., when the Bond

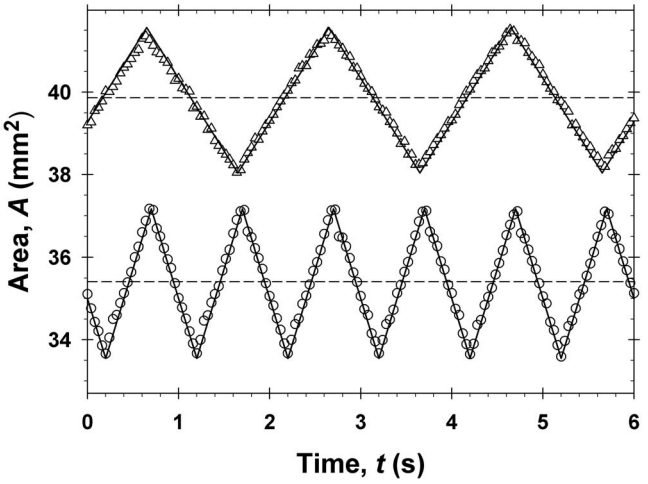

FIG. 5. Triangle waveform of area oscillations for aqueous drop in air with period of 1 s (circles) and period of 2 s (triangles). The solid lines represent the best fit to the data with triangle function.

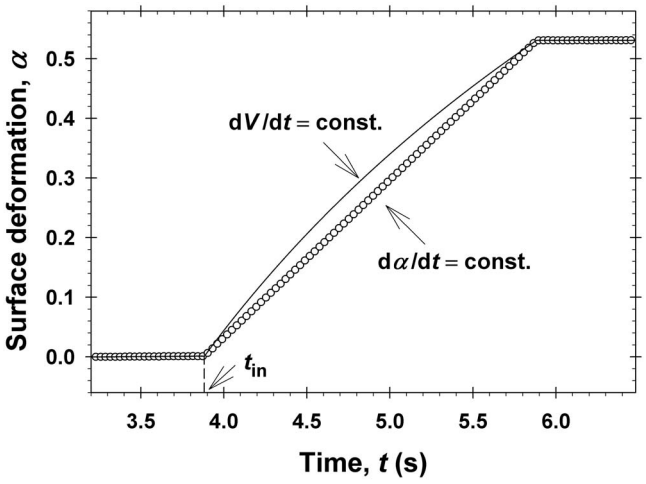

FIG. 6. Surface deformation, α, as a function of time, t, for an expanding water drop immersed in 5 mPa s PDMS. The solution contains 0.1 mM SDS and 150 mM NaCl. The circles represent measured values of α, produced with $\dot{\alpha}=0.26\ \mathrm{s}^{-1}$, as explained in Sec. II B, the solid line shows the curve $\alpha(t)$ corresponding to the regime $dV/dt=$const.

number[9] is small) the drop shape is very close to a spherical segment with radius, R_s, height, H_s, and radius of the drop base circumference, R_b. In this case the interfacial tension can be determined by measuring the instantaneous value of the pressure difference across the interface, P_c (capillary pressure), and the drop radius only.

For a drop of spherical shape hanging on the flat tip of a capillary, the application program running on the main PC calculates in real time the parameters of the best circumference passing through the contour of the drop image. Determining in this way the most probable value of R_s, and knowing R_b from optical observation, we can calculate the instantaneous values of the drop height, H_s volume, V_s, and area, A_s, from the relationships,

$$R_b^2 = H_s(2R_s - H_s), \quad 3V_s = \pi H_s^2(3R_s - H_s), \quad A_s = 2\pi R_s H_s. \tag{1}$$

At fixed contact line (R_b=const) the total differentials of the drop volume and area can be calculated from Eq. (1)

$$dV_s = \pi R_s H_s dH_s, \quad dA_s = 2\pi H_s dH_s, \quad R_s dA_s = 2dV_s. \tag{2}$$

The last equation shows that for small deformations (i.e., R_s almost constant) to leading order of magnitude, the area change, dA_s, is proportional to the volume change, dV_s. In this case the waveforms of the drop volume and area oscillations are similar in shape and the amplitude of the area waveform can be calculated prior to the oscillations and used as an input parameter for the application program.

The spherical drops are typically much smaller in volume than the pendant drops. For example, an aqueous drop, formed on a tip of radius 0.9 mm, should have a radius of the order of 1 mm to acquire a good spherical shape in air. Such a drop has a volume of about 3 μl only and an area of about 9 mm^2. Realization of relative surface deformation of 5%, in 1024 steps per period, requires step volume change of 0.2 nl.

4. Expanding/contracting spherical drops

If the deformation $\alpha \equiv dA_s/A_s$ is small, i.e., dA_s is proportional to dV_s [see Eq. (2)], a constant rate of drop volume change dV_s/dt is sufficient to obtain constant rate of surface deformation $\dot{\alpha} \equiv (dA_s/dt)/A_s$. For larger, arbitrary drop deformations (larger than 5%) the rate of surface deformation, $\dot{\alpha}$, is no longer linear function of the drop volume change. To obtain the most appropriate regime of drop deformation $\dot{\alpha}$=const one must control in a special way $V_s(t)$. The necessary condition can be obtained from

$$\dot{\alpha}dt = \frac{dA_s}{A_s} = \frac{dH_s}{R_s} = d\ \ln(R_b^2 + H_s^2) \tag{3}$$

following from Eqs. (1) and (2). Integrating Eq. (3) with initial condition $H_s(0)=H_{s,0}$ and $\dot{\alpha}$=const one obtains the necessary relations between the drop volume, V_s, at each moment, t and the initial drop height, $H_{s,0}$,

$$V_s = \pi H_s(3R_b^2 + H_s^2)/6, \tag{4}$$

where

$$H_s^2(t) = (R_b^2 + H_{s,0}^2)\exp(\dot{\alpha}t) - R_b^2.$$

In Eq. (4) the case of $\dot{\alpha}>0$ corresponds to expansion while $\dot{\alpha}<0$ means contraction. The circles in Fig. 6, falling on a straight line, correspond to this mode of surface deformation. One might be tempted to use the regime of constant rate of drop volume change, dV/dt=const, instead of the technically more difficult regime with $\dot{\alpha}$=const. The respective dependence is also shown in Fig. 6 by solid curve. The difference between the two regimes is obvious. One could use in principle either of them but the interpretation of the rheological equations is much simpler in the case $\dot{\alpha}$=const.

The drop area can be kept constant after the deformation is stopped (Fig. 6). To achieve that, the IU and the application program use a feedback control of the drop radius in real time. This mode of operation allows one to measure the pure relaxation of the surface stress, τ_s, after the initial deformation (expansion or contraction) is arrested. In this way, effects such as diffusion of surfactant from the bulk, possible surface reactions or conformational changes in the adsorbed molecules can be conveniently studied.[4,5]

C. Calculation of interfacial tension and rheological parameters

In the case of *deformed drops* or bubbles, the stored image files are postprocessed by the software DSA1 to calculate $A(t)$ and $\sigma(t)$. The time interval of data acquisition is 40 ms for a standard CCD camera with 25 frames/s. If faster registration is needed, a high-speed camera could be used. Because of the good sine waveforms of area oscillations with a single frequency ω (see Fig. 3), the measured area and interfacial tension can be presented as follows:[7]

$$A(t) = A_m\{[1 + \alpha_a \exp(i\omega t)]\}, \quad \sigma(t) - \sigma_m = E^*(\omega, \alpha_a) \times[\alpha_a \exp(i\omega t)], \tag{5}$$

where i is the imaginary unit, A_m is the mean value of the drop area, α_a is the complex amplitude of the surface deformation, σ_m is the mean value of the interfacial tension, and $E^*(\omega, \alpha_a)$ is the complex interfacial modulus. For linear systems (viz., at small amplitudes α_a), the complex modulus is a function of the frequency ω only, and the real and imaginary parts of E^* are called elastic modulus, $E'(\omega)$, and loss modulus, $E''(\omega)$, respectively.[7] The product $\eta_{app}(\omega) \equiv \omega E''(\omega)$ is usually called apparent dilatational surface viscosity.[5] At a given frequency, the time series of area and interfacial tension data are processed with a simple linear regression to determine A_m, α_a, σ_m, and E^*, and subsequently used to calculate the rheological parameters E', E'', and η_{app}. For other types of waveforms, which contain more than one frequency, the user can perform Fourier analysis of the area and interfacial tension time series to obtain the rheological parameters of the studied system.

In the case of *small spherical drops*, the pressure, P, at the position of the pressure transducer is calculated from the following expression:

$$P = P_{air} + \rho_{out} g H_{out} + \rho_{out} g H_s + P_c - \rho_{inn} g H_s - \rho_{inn} g H_{inn}, \tag{6}$$

where P_{air} is the atmospheric pressure, g is the gravity acceleration, ρ_{out} and ρ_{inn} are the mass densities of the outer and inner phases, respectively, H_{out} is the submersion depth of the capillary tip in the outer phase, H_{inn} is the vertical distance from the position of the pressure transducer to the capillary tip, and $P_c = 2\sigma/R_s$ is the capillary pressure. The parameters H_{inn} and H_{out} are constants, which are measured with high accuracy before starting the actual experiment. When the outer phase is air, ρ_{out} is assumed to be zero in Eq. (6). Note that the pressure transducer measures the pressure difference, $\Delta P \equiv P_{air} - P$. Taking the total differential of Eq. (6) at fixed contact line, and eliminating from the obtained result the differentials of H_s and R_s by using Eq. (2), we derive the following relationship:

$$d\sigma = \left[\sigma\left(1 - \frac{R_s}{H_s}\right) + (\rho_{inn} - \rho_{out}) g \frac{R_s^2}{2}\right] d\alpha - \frac{R_s}{2} d\Delta P. \tag{7}$$

Thus in the case of spherical drop oscillations with small amplitudes and given frequency, it is sufficient to calculate the complex amplitude of the pressure difference, P_a, and to use the leading order terms in Eq. (7) and the definition (5) for calculating the complex modulus, E^*,

$$E^* = \sigma_0\left(1 - \frac{R_{s,0}}{H_{s,0}}\right) + (\rho_{inn} - \rho_{out}) g \frac{R_{s,0}^2}{2} - \frac{R_{s,0} P_a}{2\alpha_a}, \tag{8}$$

where the subscript "0" indicates that the value of the respective quantity is taken in the initial moment. Note that Eq. (8) does not include terms corresponding to Poiseuille and intrinsic system contributions[12,15] because these contributions have not been found significant with the used construction in the specified frequency range below 1 Hz. Due to its simplicity, Eq. (8) can be used for real-time data processing. For other types of waveforms (square, triangle, sawtooth, etc.) the user can perform Fourier analysis of the area and pressure time series and apply Eq. (8) to calculate E^*. Equation (8) shows that if one works with hemispherical drops, i.e., if $R_{s,0} = H_{s,0}$ the first term in Eq. (8) is zero so that the initial value of the interfacial tension, σ_0, is not necessary for calculating E^*. Therefore additional measurements of σ_0 are not needed.

An alternative approach for performing interfacial rheology[5,16] is to postulate *a priori* the type of the rheological model. The most popular ones are the Kelvin–Voigt model with surface elasticity, E_V, and viscosity, η_V, and the Maxwell model with surface elasticity, E_M, and viscosity, η_M. These models are described by the following equations:[5]

$$\tau_s = E_V \alpha + \eta_V \dot{\alpha} \quad \text{(Kelvin – Voigt)}, \tag{9a}$$

$$\frac{\dot{\tau}_s}{E_M} + \frac{\tau_s}{\eta_M} = \dot{\alpha} \quad \text{(Maxwell)}, \tag{9b}$$

where $\tau_s = \sigma - \sigma_0$ and $\dot{\tau}_s = d\sigma/dt$ are the surface stress and rate of surface stress, respectively.

Equation (9) shows that the regime of constant rate of surface deformation, $\dot{\alpha}$, is the most appropriate for measuring surface elasticity and viscosity. For example, the linear plot of the surface stress, τ_s, as a function of ω has a slope E_V and an intercept $\eta_V \dot{\alpha}$ for the Kelvin–Voigt model, see Eq. (9a). After integration of the Maxwell Eq. (9b) with respect to time, one derives

$$\dot{\alpha}(t - t_{in}) = \frac{1}{E_M} \tau_s(t) + \frac{1}{\eta_M} \int_{t_{in}}^{t} \tau_s dt, \tag{10}$$

where t_{in} is the initial time of the drop expansion or contraction. The linear regression of the measured surface stress by Eq. (10) gives the values of the rheological parameters E_M and η_M. The integral form of the Maxwell law, Eq. (10), is more stable for data processing than the respective differential form, Eq. (9), because the numerical differentiation is replaced by numerical integration. The solution of Eq. (9) for known $\alpha(t)$ can be also used for data processing but it leads to a nonlinear regression model for E_M and η_M.[5]

III. ILLUSTRATIVE EXPERIMENTAL RESULTS AND DISCUSSIONS

A. Materials

To demonstrate several of the modes of operation of our instrument, we performed measurements with aqueous solutions of the anionic surfactant sodium dodecyl sulfate (SDS) (from Acros, USA), cationic surfactant cetyl trimethyl am-

monium bromide (CTAB) (from Sigma), and milk proteins β-casein (Sigma) and β-lactoglobulin (β-LG) (Sigma). Sodium chloride (NaCl) (Merck) was added to some of the solutions in a concentration, as specified below for each case. Phosphate buffer (Sigma) was used for the β-casein solutions. We used de-ionized water from a milli-Q purification system (Millipore, USA), which was additionally degassed for the pressure measurements.

As oil phases we used n-hexadecane (Merck, Germany), 5 and 50 mPa s PDMS (Merck), and soybean oil (SBO) (food grade). Hexadecane and SBO were purified from surface active contaminants by passing these oils through column filled with alumina adsorbent.

All parts of the instrument contacting with the studied solutions and the glassware were cleaned with an alcoholic base solution and rinsed abundantly with de-ionized water.

B. Experimental results

1. Comparison of the methods

It is well known from literature[7,10] that measuring large interfacial moduli E' and E'', is much easier because the errors in the interfacial tension calculations are smaller than the amplitudes of the interfacial tension oscillations. To demonstrate the capabilities of our instrument, we oriented our measurements to more "difficult" systems, which have small values of E' and E''. As appropriate low molecular mass surfactant we chose the ionic surfactant SDS, for which the two-dimensional equation of state and the adsorption isotherm are known.[27] To diminish the role of possible impurities, we added 150 mM NaCl to the SDS solutions.[27,28] The values of E' and E'' were measured at several SDS concentrations, by using two different procedures: (i) oscillations of small spherical drops and interfacial tension calculation from the measured pressure (SDA); and (ii) oscillations of well-deformed drops and interfacial tension calculations using a fit to the drop shape by Laplace equation of capillarity (DSA). Both types of experiment gave the same values of E' in the frame of the experimental error—see Fig. 7(a), where the dependence of E' on the oscillation period is shown for solution of 0.3 mM SDS+150 mM NaCl. The measured values of the loss modulus, E'', also coincided in the frame of the experimental error, see Fig. 7(b). Measurements at other concentrations of SDS (0.1 and 0.05 mM) also showed a reasonable agreement between the values of the moduli, measured by the DSA and SDA methods.

Using the procedure for a drop expansion with $\dot{\alpha}$ =const and processing the obtained experimental dependence of the surface tension, σ, on surface deformation, α, with the Kelvin–Voigt model, Eq. (9), the values of the elasticity, E_V, were obtained and are plotted in Fig. 7(a) for 0.3 mM SDS+150 mM NaCl solutions. To compare the result obtained by periodic oscillations with period $T=2\pi/\omega$ with result obtained by continuous deformation for time t_{exp}, we have to define a quantity in the continuous expansion having the meaning of a period. We have taken as such quantity $4t_{exp}$, i.e., we consider the process of surface expansion with a rate $\dot{\alpha}$ for a time t_{exp} as equivalent to a quarter of oscillation with a period $4t_{exp}$ and amplitude $\alpha = \dot{\alpha} t_{exp}$. It was shown in Ref. 5 that the values of E' and E_V are equal for purely elastic interfaces and that for soluble surfactants the elastic modulus, E', and the elasticity, E_V, are close to each other when the interfacial viscosity is small.[5] These conclusions are confirmed by our experimental results [see Fig. 7(a)]. The value of η_V was too small to be determined accurately and, for this reason, is not shown in Fig. 7(b).

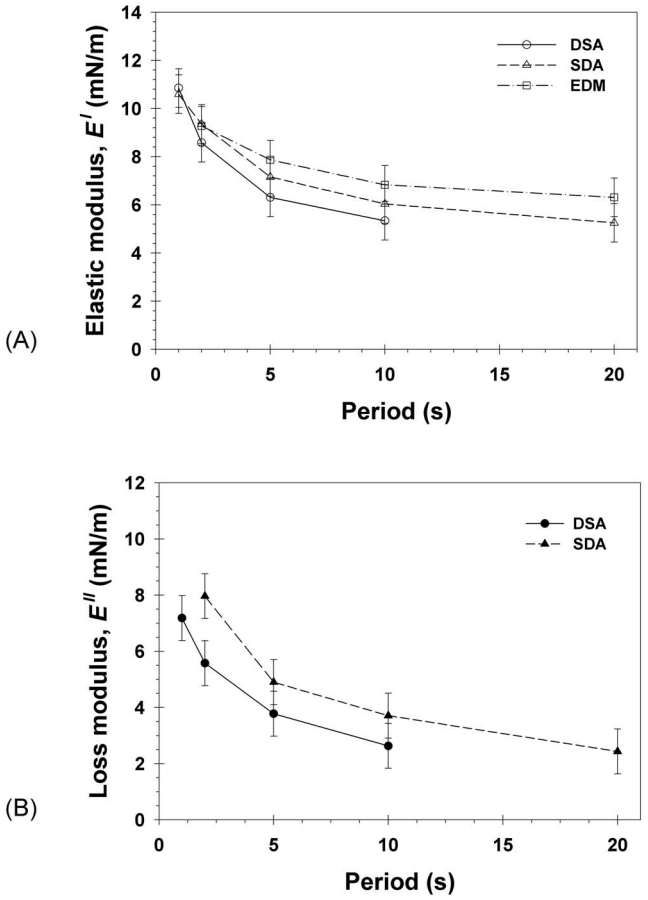

FIG. 7. (a) Elastic modulus, E', as a function of the period of oscillations for 0.3 mM SDS+150 mM NaCl and the respective value of the elasticity, E_V, of the Kelvin–Voigt model obtained from the experiments with expanding drops. (b) Loss modulus, E'', as a function of the frequency of oscillations for the same solution. Results from oscillations of spherical drops (SDA) and from oscillations of deformed drops (DSA) are compared.

2. Measurements with viscous phases and small mass density difference

If the two phases have similar mass densities, e.g., water and silicone oil (PDMS), measurements of interfacial tension by DSA is possible with very large drops only (e.g., >100 μl in volume). When applying sine oscillations to such drops, the area versus time curves obey a perfect sine function (as illustrated in Fig. 3), but nevertheless, one could obtain wrong results for the rheological parameters. As illustration, in Fig. 8 we compare values of E' and E'', obtained by using DSA and SDA methods, for oscillating water drops (with 0.1 mM SDS+150 mM NaCl) in silicone oil with viscosity 5 mPa s. The values obtained by the two methods coincide for the long periods of oscillation; however, significant differences are observed for E' at shorter periods of

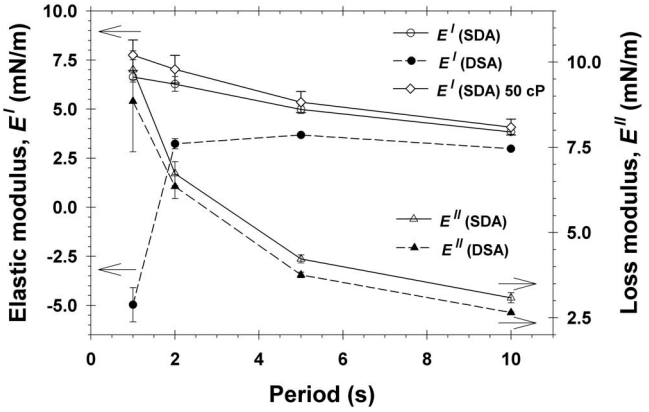

FIG. 8. Experimental values of the elastic modulus, E' (circles, diamonds, left y-axis), and the loss modulus, E'' (triangles, right y-axis), measured for 0.1 mM SDS+150 mM NaCl solution (inner phase). The outer phase is 5 mPa s PDMS except for one series (diamonds) where 50 mPa s PDMS is used. The empty symbols represent results obtained using spherical drops (SDA) and the filled symbols correspond to the detection of the interfacial tension from DSA.

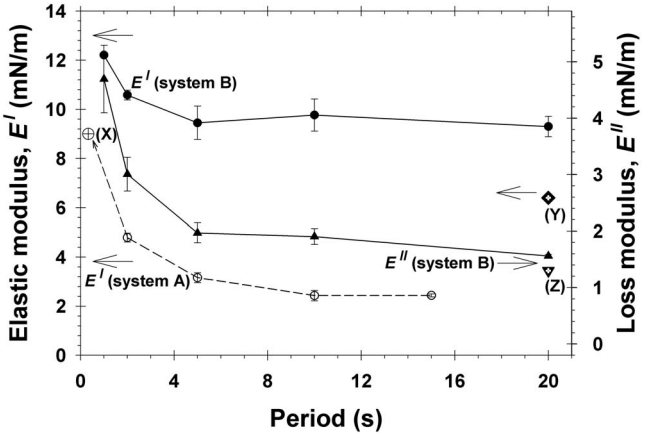

FIG. 9. Experimental values for the elastic modulus, E' (circles), and the loss modulus, E'' (triangles), as a function of the period of oscillations for bubbles immersed in 0.3 mM CTAB solution (system A—empty symbols), and for n-hexadecane drops aged for 30 min in 8.5×10^{-4} wt % $\beta-$casein solution in phosphate buffer with pH=7 and ionic strength 100 mM (system B—filled symbols). For comparison, points corresponding to literature data are shown: E' for 0.1 mM CTAB from Ref. 30 (crossed circle X); E' (Y—diamond); and E'' (Z—triangle down) for n-hexadecane drops aged for 30 min in 8.5×10^{-4} wt % $\beta-$casein solution in phosphate buffer with pH=7 and ionic strength 100 mM from Ref. 31.

1 and 2 s. Furthermore, the elastic modulus, E', determined by DSA has negative values at the shortest period of $T=1$ s (see Fig. 8), which is obviously a nonphysical result.

The reasons for the incorrect measurements of the rheological parameters using DSA under these conditions (large drops, similar mass densities of the liquids, not-very-large periods of oscillations) could be as follows: (1) imprecise determination of interfacial tension due to insufficient drop deformation, and/or (2) significant viscous stress in the drop interior, which affects drop shape, thus leading to wrong results for interfacial tension.[8,9] The agreement between the values at larger periods indicates that the problems observed with DSA at short periods are caused predominantly by viscous effects.[4,29] Note that the viscous friction is most pronounced in the narrowest region of the drop neck. On the other side, the measured value of the surface tension is most sensitive to drop shape in this region. Only at sufficiently slow oscillations, the viscous effects in drop interior become negligible and the measured values of E' with DSA become acceptable (and coincide with those measured by SDA).

In contrast, when using oscillations of spherical drops with a pressure detection (SDA), the measured values of the elastic modulus, E', are reasonable in the entire frequency range used (from 0.1 to 1 Hz, cf. also Figs. 7 and 8). To check whether even more viscous oils could be used in such measurements, we performed additional experiments with the same surfactant solution and silicone oil of higher viscosity, 50 mPa s. The values of E' and E'' for 5 and 50 mPa s silicone oils, as determined with SDA, coincide within the experimental error (only E' is shown in Fig. 8 to keep this figure sufficiently simple and readable), which is an additional proof that SDA works properly and gives physically meaningful results for such viscous oils—indeed, the surface rheological parameters are not expected to vary significantly upon not-very-large changes in viscosity (5–50 mPa s in this particular example), just as observed in the SDA measurements. Note that the values determined by DSA for 50 mPa s oil (not shown in Fig. 8) were very different from all results shown in Fig. 8, which confirms the conclusion that viscous friction makes the DSA method inapplicable to viscous oils.

From the presented experimental data we could conclude that the rheological parameters for interfaces involving viscous oils can be measured correctly for moderate oil viscosity, up to 50 mPa s, and oscillation periods longer than 1 s, by using spherical drops with pressure detection, where the DSA method might be inapplicable due to viscous effects in drop interior.

3. Comparison with literature data

Figure 9 illustrates our results for E' and E'' for oscillation period in the range of 1–20 s (viz., frequency 1–0.05 Hz), for two different systems: (A) oscillating deformed bubbles in solution of 0.3 mM CTAB; and (B) oscillating deformed drops of n-hexadecane immersed in 8.5×10^{-4} wt % $\beta-$casein solution in phosphate buffer (ionic strength 100 mM, pH=7) after 30 min aging. Fruhner and Wantke[30] studied oscillating spherical bubbles in CTAB solutions at frequency ≥ 3 Hz (up to 300 Hz). Their value for E' at frequency 3 Hz fits well on the trend obtained by us at lower frequencies. Freer *et al.*[31] performed oscillations with hexadecane drops in β-casein solution (same as our system B) at a single frequency of 0.05 Hz (period 20 s) and determined $E'\approx 6.5\pm0.5$ mN/m and $E''\approx 1.2$ mN/m, which are close to our results, especially for E'' (see Fig. 9).

4. Expanding drop measurements

To illustrate the application of the EDM, we performed experiments with 0.01 wt % solution of globular protein β-lactoglobulin+10 mM NaCl. Our experiments showed that the characteristic diffusion time of this protein is much longer than the time of expansion of the drop surface (1–10 s) and, therefore, the protein behaves as insoluble during the

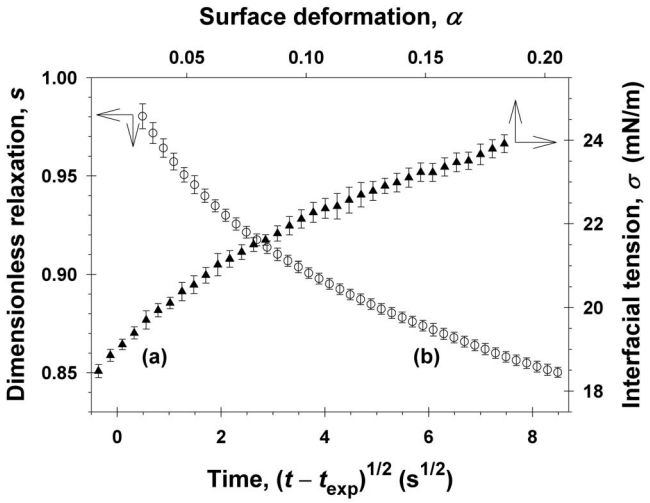

FIG. 10. Combined plots of (a) dependence of the interfacial tension, $\sigma(t)$, on the surface deformation, $\alpha(t)$, for expansions of SBO drops immersed in 0.01 wt % β-LG+10 mM NaCl solution—the full triangles correspond to the right-hand-side ordinate and top abscissa. (b) The dimensionless stress after the expansions, $s(t)$, is shown as a function of $(t-t_{\mathrm{exp}})^{1/2}$—empty circles correspond to the left-hand-side ordinate and bottom abscissa.

expansion period. In such a case, the change in protein adsorption, $\Delta\Gamma$, is related to the surface deformation, α, by the equation[5] $\Delta\Gamma(t)/\Gamma_0=-1/\alpha$, and the drop expansion or contraction experiments can be used for obtaining the two-dimensional equation of state, $\sigma=\sigma(\Gamma)$. Therefore, such experiments give similar information to that obtained by the Langmuir trough method.

Figure 10 illustrates the measured dependence of the interfacial tension, σ, as a function of the surface deformation, α, for expansions of SBO drops immersed in 0.01 wt % β-LG solution. The experimental procedure was the following. After the initial drop formation we waited 30 min to reach surface saturation. To check for possible nonequilibrium effects in the equation of state, we used different expansion rates, $\dot{\alpha}$, and expansion times, t_{exp}, combined in such a way that the total deformation, α, be the same, $\alpha=0.18$. The values $\sigma(\alpha)$ shown in Fig. 10 are averaged over all measurements at different rates of surface deformation and the error bars represent the deviation of the experimental points. The result shows that the experimental curves $\sigma=\sigma(\alpha)$ obtained with different values of $\dot{\alpha}$ collapsed to a single master curve $\sigma(\alpha)$, which means that $\sigma(\alpha)$ and the respective equation of state $\sigma(\Gamma)$ do not depend on the rate of surface deformation. This confirms the conclusion reached in Refs. 32 and 33 that the surface pressure depends (at constant temperature) only on the instantaneous adsorption, Γ, no matter how it was reached.

After drop expansion, the feedback system was switched on to maintain the drop surface area constant. The measured interfacial tension relaxed slowly to its equilibrium value because of the slow diffusion of protein molecules to the surface. The dimensionless stress during relaxation, $s(t)=[\sigma(t)-\sigma_0]/(\sigma_{\mathrm{max}}-\sigma_0)$, where σ_{max} is the maximum value of the interfacial tension, is also plotted in Fig. 10. The shown values of $s(t)$ are averaged over all experiments and the error bars correspond to the deviation of the experimental points. All curves are shifted by the respective deformation time, t_{exp}, in order to have the same zero of the abscissa axes. A very good common relaxation curve is obtained (see Fig. 10), which is not surprising because the values of α and σ at the end of expansion are the same in all these experiments so that the relaxation curves are expected to coincide. From the obtained curve we calculated the characteristic diffusion relaxation time, $t_{\mathrm{rel}}\approx 47$ s. This is much longer than the expansion time, t_{exp}, which supports our assumption, made above, that the diffusion is slow. The fact that we obtained master curves both for the expansion and the relaxation processes confirms also the correctness of our method and procedure.

In summary, the presented instrument allows very precise shape of the drop area perturbations due to appropriate piezodriven system, controlled with a very high time resolution (up to 1024 points/s) and small volume step (around 0.1 nl). Accurate synchronization is ensured, and real-time measurements and feedback control of the drop volume and area are implemented for the SDA and EDM methods. The combination of several complementary methods for determination of the interfacial tension and interfacial rheological parameters in a single instrument, allows fast and effective selection of most suitable procedure for each specific system. For example, EDM and SDA measurements can be applied to liquids with very small mass density difference and/or with relatively high viscosity (not offered by other instruments). The EDM can be applied to study insoluble monolayers, by using a very small sample volume, while the feedback drop area control allows accurate measurements of the surface tension relaxation.

ACKNOWLEDGMENTS

The authors are deeply indebted to Professor Ivan B. Ivanov for his continuous support and encouraging, and for his valuable suggestions and comments throughout the entire process of instrument development. This study was supported by Krüss GmbH, Hamburg, Germany.

[1] *Food Emulsions and Foams—Interfaces, Interactions and Stability*, 227 ed., edited by E. Dickinson and J. M. R. Patino (RSC, London, 1999).
[2] S. A. Koehler, S. Hilgenfeldt, E. R. Weeks, and H. Stone, Phys. Rev. E **66**, 040601 (2002).
[3] N. D. Denkov, V. Subramanian, D. Gurovich, and A. Lips, Colloids Surf., A **263**, 129 (2005).
[4] *Drops and Bubbles in Interfacial Research*, edited by D. Möbius and R. Miller (Elsevier, Amsterdam, 1998).
[5] I. B. Ivanov, K. D. Danov, K. P. Ananthapadmanabhan, and A. Lips, Adv. Colloid Interface Sci. **114**, 61 (2005).
[6] G. Loglio, U. Tesei, and R. Cini, Rev. Sci. Instrum. **59**, 2045 (1988).
[7] J. Lucassen and M. van den Tempel, Chem. Eng. Sci. **27**, 1283 (1972).
[8] Y. Rotenberg, L. Boruvka, and A. W. Neumann, J. Colloid Interface Sci. **93**, 169 (1983).
[9] M. Hoorfar and A. W. Neumann, Adv. Colloid Interface Sci. **121**, 25 (2006).
[10] J. Benjamins, A. Cagna, and E.-H. Lucassen-Reynders, Colloids Surf., A **114**, 245 (1996).
[11] M. A. Cabrerizo-Vilchez, H. A. Wege, J. A. Holgado-Terriza, and A. W. Neumann, Rev. Sci. Instrum. **70**, 2438 (1999).
[12] V. I. Kovalchuk, J. Kragel, E. V. Aksenenko, G. Loglio, and L. Liggieri, in *Novel Methods to Study Interfacial Layers*, edited by D. Möbius and R. Miller (Elsevier, Amsterdam, 2001), p. 485.
[13] G. Loglio, U. Tesei, P. Pandolfini, and R. Cini, Colloids Surf., A **114**, 23 (1996).

[14] K. D. Wantke, K. Lunkenheimer, and C. Hempt, J. Colloid Interface Sci. **159**, 28 (1993).
[15] L. Liggieri and F. Ravera, in *Drops and Bubbles in Interfacial Research*, edited by D. Möbius and R. Miller (Elsevier, Amsterdam, 1998), p. 239.
[16] T. Horozov, K. Danov, P. A. Kralchevsky, I. B. Ivanov, and R. Borwankar, Proceedings of the First World Congress on Emulsion, Paris, France, 1993, Paper No. 3-20-137.
[17] R. Nagarajan and D. T. Wasan, J. Colloid Interface Sci. **159**, 164 (1993).
[18] I. B. Ivanov, S. R. Russev, L. Lyutov, V. Vulchev, K. G. Marinova, N. Alexandrov, D. T. Dimitrova, A. Bunz, C. Bilke-Krause, and C. Gerber, German Patent No. 10 2004 040 336.8 (August 2004).
[19] M. E. Leser, S. Acquistapace, A. Cagna, A. V. Makievski, and R. Miller, Colloids Surf., A **261**, 25 (2005).
[20] J. Hyde, *USB Design by Example: A Practical Guide to Building I/O Devices* (Wiley, New York, 1999).
[21] Analog Devices Inc. (www.analog.com).
[22] MetaLink Corporation (www.metaice.com/ASM51/ASM51.htm).
[23] Future Technology Devices International Ltd. (www.ftdichip.com).
[24] I. B. Ivanov, K. G. Marinova, V. Vulchev, D. T. Dimitrova, K. D. Danov, N. D. Denkov, S. R. Russev, L. Lyutov, N. Alexandrov, German Patent No. 10 2007 056 669.9 (November 2007).
[25] D. M. Sztukowski and H. W. Yarranton, Langmuir **21**, 11651 (2005).
[26] R. Miller, G. Loglio, U. Tesei, and K.-H. Schano, Adv. Colloid Interface Sci. **37**, 73 (1991).
[27] T. D. Gurkov, D. T. Todorova, K. G. Marinova, C. Bilke-Crause, C. Gerber, and I. B. Ivanov, Colloids Surf., A **261**, 29 (2005).
[28] P. A. Kralchevsky, K. D. Danov, V. L. Kolev, G. Broze, and A. Mehreteab, Langmuir **19**, 5004 (2003).
[29] D. A. Edwards, H. Brenner, and D. T. Wasan, *Interfacial Transport Processes and Rheology* (Butterworth-Heinemann, Boston, 1991).
[30] H. Frühner and K. D. Wanke, Colloids Surf., A **114**, 53 (1996).
[31] E. M. Freer, K. S. Yim, G. G. Fuller, and C. J. Radke, J. Phys. Chem. B **108**, 3835 (2004).
[32] T. D. Gurkov, S. C. Russev, K. D. Danov, I. B. Ivanov, and B. Campbell, Langmuir **19**, 7362 (2003).
[33] D. E. Graham and M. C. Phillips, J. Colloid Interface Sci. **70**, 415 (1979).